

A photometric study of the K-type contact binary EI CVn *

Yuan-Gui Yang

School of Physics and Electronic Information, Huaibei Normal University, Huaibei 235000, China;
yygcn@163.com

Received 2010 June 12; accepted 2010 August 12

Abstract We present charge-coupled device (CCD) photometry for the short-period K-type binary EI CVn, observed on 2009 February 28 at the Xinglong Station of National Astronomical Observatories, Chinese Academy of Sciences. By using the Wilson-Devinney program, the photometric solution was first deduced from our *VR* observations. The results show that EI CVn is a W-type weak-contact binary with a mass ratio of $q_{\text{ph}} = 0.2834(\pm 0.0010)$ and an overcontact degree of $f = 20.0\%(\pm 0.7\%)$. The distorted light curves were modeled by a dark spot on the cool primary component, whose area was up to 1.9% of the area of the primary. Based on the period analysis, it is found that there exists a weak secular decrease at a rate of $dP/dt = -3.11(\pm 0.03) \times 10^{-7} \text{ d yr}^{-1}$, which may be attributed to mass transfer from the primary to the secondary. With mass transfer occurring, the separation between both components will shrink, which may cause the degree of overcontact to increase. Therefore, the weak-contact binary EI CVn may evolve into a deep-contact configuration.

Key words: stars: binaries: close — stars: binaries: eclipsing — stars: individual: EI CVn

1 INTRODUCTION

The variable star EI CVn (=GSC 2548–936, $\alpha_{\text{J2000.0}} = 14^{\text{h}}02^{\text{m}}05.57^{\text{s}}$ and $\delta_{\text{J2000.0}} = +34^{\circ}02'39.''97$) was discovered by the Robotic Optical Transient Search Experiment I (ROTSE-I) All-Sky Surveys (Akerlof et al. 2000). This binary was classified as an EW-type binary with a period of $P = 0.260775^{\text{d}}$ and an unfiltered ROTSE magnitude of 11.91^{m} . Stephenson (1986) derived the spectral type of K5. Then Beers et al. (1994) listed it as an emission-line candidate. The color indexes are $J - H = +0.567$ and $H - K = +0.124$ (Gettel et al. 2006). Blättler & Diethelm (2003) observed this star and obtained 138 unfiltered CCD observations. The light curve of EI CVn varies approximately from 11.8^{m} to 12.5^{m} . Based on their observations and ROTSE-I data, they published 12 light minimum times and revised its orbital period to 0.260768^{d} , indicating that the orbital period may be variable. Unfortunately, the epoch time of HJD 2452694.3796 is a secondary eclipse rather than a primary one, identified by our new photometry. Seen from the folded light curve of EI CVn (Blättler & Diethelm 2003), one cannot decide which one is the primary or the secondary due to large scatter and almost equal depths for both eclipses. Although some light minimum times were

* Supported by the National Natural Science Foundation of China.

observed, no photometric elements of this binary have been published up to now. To study the evolutionary status and chromospheric activity of the late-type eclipsing binary 1RX J201607.0+251645 (Li et al. 2009), EI CVn was included in the observing program.

2 OBSERVATIONS

New Photometry of EI CVn was carried out on 2009 February 28 using the 60-cm telescope at the Xinglong Station of the National Astronomical Observatories, Chinese Academy of Sciences (NAOC). The photometer was equipped with a 1024×1024 pixel CCD camera. Each pixel subtends a projected angle on the sky of $0.996''$, which results in a field of view of $17' \times 17'$. All observed CCD images were reduced by means of the IRAF package in the standard fashion. The stars GSC 2548–79 ($\alpha_{J2000.0} = 14^{\text{h}}01^{\text{m}}30.70^{\text{s}}$ and $\delta_{J2000.0} = +34^{\circ}00'11.89''$) and GSC 2548–10 ($\alpha_{J2000.0} = 14^{\text{h}}01^{\text{m}}57.82^{\text{s}}$ and $\delta_{J2000.0} = +34^{\circ}00'16.7''$) were selected as the comparison and check stars, respectively. In the observing process, typical exposure times were 60 s for the V band and 30 s for the R band. Table 1 lists all individual observations, i.e., heliocentric Julian dates (HJD) versus the magnitude differences between the variable and the comparison (Δm), which are displayed in Figure 1. The phases were calculated with a revised period of 0.26076667^{d} from Equation (1). For each of the VR light curves, the mean error between the magnitude of the comparison and that of the check is less than 0.005^{m} . EI CVn possesses an EW-type light curve displayed in Figure 1. The variable light amplitudes in the VR bands are 0.66^{m} and 0.71^{m} , respectively. The primary eclipses are slightly deeper than the secondary eclipses, up to 0.064^{m} for the V band and 0.044^{m} for the R band. There exists an unequal height between the two maxima, i.e., the O’Connell effect (Milone 1968; Davidge & Milone 1984). Max.I is brighter than Max.II by up to 0.036^{m} for the V band and 0.017^{m} for the R band.

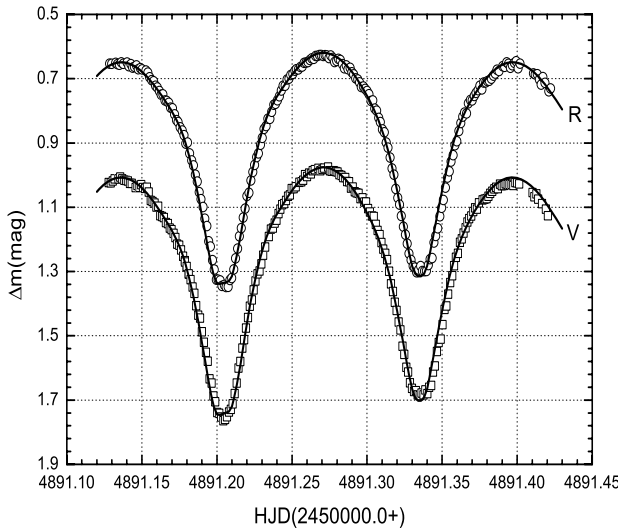


Fig. 1 VR observations of EI CVn, observed on 2009 February 28, using the 60-cm telescope at the Xinglong Station of NAOC. The solid lines were plotted by generating a photometric solution that follows a dark spot.

Table 1 *VR* Observations of the Eclipsing Binary EI CVn

JD (Hel.)	<i>V</i> band		<i>R</i> band		
	$\Delta(m)$	JD (Hel.)	$\Delta(m)$	JD (Hel.)	$\Delta(m)$
2454891.1279	1.023	2454891.2714	0.978	2454891.1285	0.653
2454891.1293	1.024	2454891.2740	0.975	2454891.1299	0.654
2454891.1306	1.018	2454891.2752	0.986	2454891.1325	0.651
2454891.1318	1.012	2454891.2765	0.988	2454891.1337	0.655
2454891.1344	1.012	2454891.2778	0.986	2454891.1350	0.656
2454891.1356	1.006	2454891.2791	0.989	2454891.1363	0.649
2454891.1369	1.012	2454891.2803	0.990	2454891.1375	0.654
2454891.1382	1.016	2454891.2816	0.999	2454891.1401	0.650
2454891.1394	1.017	2454891.2829	1.001	2454891.1413	0.661
2454891.1407	1.018	2454891.2841	1.008	2454891.1426	0.655
2454891.1420	1.026	2454891.2854	1.008	2454891.1439	0.665
2454891.1432	1.026	2454891.2867	1.020	2454891.1451	0.663
2454891.1458	1.039	2454891.2880	1.021	2454891.1464	0.659
2454891.1470	1.032	2454891.2892	1.040	2454891.1476	0.670
2454891.1483	1.038	2454891.2905	1.037	2454891.1489	0.667
2454891.1495	1.030	2454891.2918	1.052	2454891.1502	0.671
2454891.1508	1.039	2454891.2930	1.055	2454891.1527	0.674
2454891.1521	1.041	2454891.2943	1.057	2454891.1540	0.681
2454891.1533	1.038	2454891.2956	1.073	2454891.1552	0.696
2454891.1546	1.053	2454891.2969	1.071	2454891.1565	0.705
2454891.1559	1.079	2454891.2981	1.084	2454891.1578	0.708
2454891.1571	1.082	2454891.2994	1.084	2454891.1590	0.722
2454891.1584	1.087	2454891.3007	1.104	2454891.1603	0.728
2454891.1597	1.099	2454891.3019	1.115	2454891.1616	0.738
2454891.1609	1.097	2454891.3032	1.127	2454891.1628	0.750
2454891.1622	1.126	2454891.3045	1.129	2454891.1641	0.749
2454891.1635	1.129	2454891.3058	1.153	2454891.1654	0.768
2454891.1647	1.132	2454891.3070	1.172	2454891.1666	0.769
2454891.1660	1.148	2454891.3083	1.185	2454891.1679	0.775
2454891.1673	1.151	2454891.3096	1.210	2454891.1692	0.790
2454891.1685	1.165	2454891.3108	1.230	2454891.1704	0.792
2454891.1698	1.170	2454891.3121	1.243	2454891.1717	0.811
2454891.1711	1.181	2454891.3134	1.263	2454891.1730	0.829
2454891.1723	1.194	2454891.3147	1.299	2454891.1742	0.835
2454891.1736	1.215	2454891.3159	1.338	2454891.1755	0.851
2454891.1749	1.218	2454891.3172	1.362	2454891.1768	0.861
2454891.1761	1.233	2454891.3185	1.396	2454891.1780	0.876
2454891.1774	1.252	2454891.3197	1.421	2454891.1793	0.902
2454891.1787	1.266	2454891.3210	1.457	2454891.1805	0.899
2454891.1799	1.286	2454891.3223	1.482	2454891.1818	0.932
2454891.1812	1.308	2454891.3236	1.532	2454891.1831	0.954
2454891.1878	1.270	2454891.3248	1.558	2454891.1843	0.970
2454891.1799	1.284	2454891.3261	1.598	2454891.1856	0.999
2454891.1812	1.307	2454891.3274	1.613	2454891.1869	1.020
2454891.1824	1.325	2454891.3286	1.646	2454891.1881	1.053
2454891.1837	1.348	2454891.3299	1.663	2454891.1894	1.075
2454891.1850	1.368	2454891.3312	1.673	2454891.1907	1.099
2454891.1862	1.406	2454891.3325	1.671	2454891.1919	1.135
2454891.1875	1.436	2454891.3337	1.684	2454891.1932	1.158
2454891.1888	1.445	2454891.3350	1.686	2454891.1945	1.206
2454891.1900	1.487	2454891.3363	1.678	2454891.1957	1.222
2454891.1913	1.520	2454891.3376	1.684	2454891.1970	1.265
2454891.1926	1.551	2454891.3388	1.668	2454891.1983	1.294
2454891.1938	1.579	2454891.3401	1.680	2454891.1996	1.325
2454891.1951	1.634	2454891.3414	1.660	2454891.2008	1.325
2454891.1964	1.647	2454891.3427	1.654	2454891.2021	1.328
2454891.1976	1.687	2454891.3439	1.613	2454891.2033	1.345
2454891.1989	1.705	2454891.3452	1.594	2454891.2048	1.342

Table 1 — *Continued.*

JD (Hel.)	<i>V</i> band		Δ (m)	<i>R</i> band			
	JD (Hel.)	Δ (m)		JD (Hel.)	Δ (m)	JD (Hel.)	Δ (m)
2454891.2002	1.739	2454891.3465	1.549	2454891.2061	1.348	2454891.3471	1.166
2454891.2015	1.741	2454891.3477	1.521	2454891.2074	1.347	2454891.3484	1.128
2454891.2027	1.753	2454891.3490	1.510	2454891.2086	1.326	2454891.3497	1.102
2454891.2042	1.764	2454891.3503	1.465	2454891.2099	1.320	2454891.3509	1.077
2454891.2055	1.760	2454891.3516	1.418	2454891.2112	1.293	2454891.3522	1.039
2454891.2067	1.752	2454891.3528	1.407	2454891.2124	1.259	2454891.3535	1.008
2454891.2080	1.737	2454891.3541	1.370	2454891.2137	1.229	2454891.3548	0.988
2454891.2093	1.729	2454891.3554	1.334	2454891.2150	1.190	2454891.3560	0.958
2454891.2105	1.712	2454891.3567	1.313	2454891.2162	1.165	2454891.3573	0.938
2454891.2118	1.680	2454891.3579	1.282	2454891.2175	1.132	2454891.3586	0.907
2454891.2131	1.647	2454891.3592	1.256	2454891.2188	1.104	2454891.3598	0.895
2454891.2143	1.600	2454891.3605	1.243	2454891.2200	1.065	2454891.3611	0.863
2454891.2156	1.580	2454891.3618	1.209	2454891.2213	1.055	2454891.3624	0.838
2454891.2169	1.538	2454891.3630	1.198	2454891.2226	1.017	2454891.3637	0.818
2454891.2181	1.512	2454891.3643	1.180	2454891.2238	0.990	2454891.3649	0.805
2454891.2194	1.476	2454891.3656	1.164	2454891.2251	0.968	2454891.3662	0.808
2454891.2207	1.443	2454891.3669	1.146	2454891.2264	0.944	2454891.3675	0.777
2454891.2219	1.408	2454891.3681	1.135	2454891.2276	0.932	2454891.3688	0.766
2454891.2232	1.388	2454891.3694	1.127	2454891.2289	0.905	2454891.3700	0.768
2454891.2245	1.357	2454891.3707	1.113	2454891.2302	0.884	2454891.3713	0.754
2454891.2257	1.329	2454891.3720	1.102	2454891.2314	0.856	2454891.3726	0.744
2454891.2270	1.307	2454891.3732	1.106	2454891.2327	0.847	2454891.3739	0.736
2454891.2283	1.298	2454891.3745	1.086	2454891.2340	0.824	2454891.3751	0.722
2454891.2295	1.276	2454891.3770	1.077	2454891.2353	0.825	2454891.3764	0.733
2454891.2308	1.249	2454891.3783	1.075	2454891.2365	0.803	2454891.3777	0.712
2454891.2321	1.224	2454891.3796	1.073	2454891.2378	0.781	2454891.3790	0.711
2454891.2346	1.191	2454891.3809	1.066	2454891.2391	0.778	2454891.3802	0.707
2454891.2359	1.168	2454891.3821	1.057	2454891.2403	0.767	2454891.3815	0.706
2454891.2372	1.165	2454891.3834	1.050	2454891.2416	0.755	2454891.3828	0.700
2454891.2384	1.149	2454891.3847	1.043	2454891.2429	0.737	2454891.3841	0.691
2454891.2397	1.140	2454891.3860	1.038	2454891.2441	0.722	2454891.3853	0.684
2454891.2410	1.120	2454891.3872	1.042	2454891.2454	0.722	2454891.3866	0.672
2454891.2422	1.106	2454891.3885	1.028	2454891.2467	0.702	2454891.3879	0.676
2454891.2435	1.092	2454891.3898	1.033	2454891.2479	0.700	2454891.3904	0.661
2454891.2448	1.089	2454891.3911	1.032	2454891.2492	0.688	2454891.3917	0.663
2454891.2460	1.079	2454891.3923	1.027	2454891.2505	0.685	2454891.3930	0.649
2454891.2473	1.066	2454891.3936	1.030	2454891.2518	0.675	2454891.3943	0.654
2454891.2486	1.062	2454891.3949	1.029	2454891.2530	0.670	2454891.3955	0.666
2454891.2498	1.042	2454891.3962	1.029	2454891.2543	0.671	2454891.3968	0.658
2454891.2511	1.042	2454891.3974	1.032	2454891.2556	0.664	2454891.3981	0.651
2454891.2524	1.036	2454891.3987	1.023	2454891.2568	0.662	2454891.3994	0.646
2454891.2549	1.022	2454891.4000	1.024	2454891.2581	0.651	2454891.4006	0.668
2454891.2562	1.021	2454891.4013	1.027	2454891.2594	0.650	2454891.4019	0.653
2454891.2575	1.016	2454891.4102	1.054	2454891.2606	0.648	2454891.4108	0.683
2454891.2587	0.999	2454891.4115	1.067	2454891.2619	0.642	2454891.4121	0.687
2454891.2600	1.004	2454891.4128	1.058	2454891.2632	0.637	2454891.4134	0.686
2454891.2613	0.994	2454891.4140	1.075	2454891.2645	0.638	2454891.4147	0.702
2454891.2625	0.996	2454891.4166	1.089	2454891.2657	0.629	2454891.4159	0.719
2454891.2638	0.986	2454891.4191	1.106	2454891.2670	0.629	2454891.4172	0.695
2454891.2651	0.983	—	—	2454891.2683	0.626	2454891.4185	0.713
2454891.2676	0.979	—	—	2454891.2695	0.626	2454891.4211	0.739
2454891.2689	0.986	—	—	2454891.2708	0.629	2454891.4223	0.730
2454891.2702	0.982	—	—	2454891.2721	0.627	—	—

3 ANALYZING PERIOD CHANGES

Using the Kwee-van Woerden (K-W) method (Kwee & van Woerden 1956), four single-color light minimum times together with their errors were determined from new observations, which are listed in Table 2. We collected another 22 CCD light minimum times from IBVS (Blättler & Diethelm 2003; Diethelm 2005, 2006, 2007, 2009; Nelson 2009; Hübscher et al. 2010), listed in Table 3. According to our new minimum times, i.e., HJD 2454891.2046(I) and HJD 2454891.3357(II), the wrong minimum types from those collected data have been revised. Based on 24 light minimum timings, a linear least-squares method leads to a new ephemeris as follows,

$$\text{Min.I} = \text{HJD } 2454891.2075(\pm 0.0009) + 0.26076667(\pm 0.00000012)E. \quad (1)$$

The calculated residuals of $O - C$ are listed in Table 3, and are displayed in the upper panel of Figure 2.

Table 2 New CCD Light Minimum Times of EI CVn

JD (Hel.)	Min.	Error	Band
2454891.20458	I	0.00011	V
2454891.20469	I	0.00011	R
2454891.33566	II	0.00010	V
2454891.33574	II	0.00009	R

Table 3 All CCD Light Minimum Times of the Eclipsing Binary EI CVn

JD (Hel.)	Epoch	Min	$O - C$	Residuals	Reference
2451304.8765	-13753.0	I	-0.0070	-0.0017	Blättler & Diethelm (2003)
2451348.8201	-13584.5	II	-0.0025	+0.0025	Blättler & Diethelm (2003)
2452655.5242	-8573.5	II	-0.0003	-0.0013	Blättler & Diethelm (2003)
2452691.5112	-8435.5	II	+0.0010	-0.0001	Blättler & Diethelm (2003)
2452691.6429	-8435.0	I	+0.0023	+0.0012	Blättler & Diethelm (2003)
2452694.3801	-8424.5	II	+0.0014	+0.0003	Blättler & Diethelm (2003)
2452694.5094	-8424.0	I	+0.0003	-0.0008	Blättler & Diethelm (2003)
2452694.6420	-8423.5	II	+0.0025	+0.0014	Blättler & Diethelm (2003)
2452721.3689	-8321.0	I	+0.0008	+0.0004	Blättler & Diethelm (2003)
2452723.3241	-8313.5	II	+0.0004	-0.0008	Blättler & Diethelm (2003)
2452723.4541	-8313.0	I	+0.0000	-0.0012	Blättler & Diethelm (2003)
2452723.5856	-8312.5	II	+0.0011	-0.0001	Blättler & Diethelm (2003)
2453045.5010	-7078.0	I	+0.0000	-0.0018	Blättler & Diethelm (2003)
2453491.4147	-5368.0	I	+0.0027	+0.0007	Diethelm (2005)
2453491.5455	-5367.5	II	+0.0031	+0.0011	Diethelm (2005)
2453809.4192	-4148.5	II	+0.0022	-0.0004	Diethelm (2006)
2454172.4083	-2756.5	II	+0.0041	+0.0030	Diethelm (2007)
2454554.8178	-1290.0	I	-0.0007	-0.0006	Nelson (2009)
2454817.0176	-284.5	II	-0.0018	-0.0007	Nelson (2009)
2454891.2046	+0.0	I	-0.0029	-0.0014	Present work
2454891.3357	+0.5	II	-0.0022	-0.0007	Present work
2454972.4364	+311.5	II	+0.0001	+0.0020	Diethelm (2009)
2454972.4345	+311.5	II	-0.0018	+0.0001	Hübscher et al. (2010)
2454972.5640	+312.0	I	-0.0027	-0.0008	Hübscher et al. (2010)

For close binaries, orbital period changes are common, which may be helpful for understanding the dynamics of binary stars and their stellar structures. Although the observed eclipse interval of EI CVn only covers 10 yr, we attempted to study the changes in its period. From the upper panel of Figure 2, the $O - C$ curve appears to show a downward parabolic curve, or part of a sinusoidal

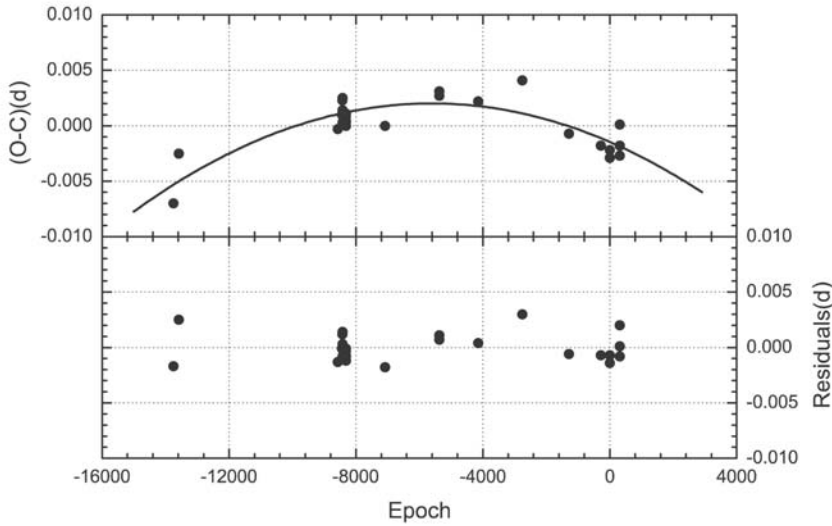


Fig. 2 $(O - C)$ curve (upper panel) and the corresponding residuals (lower panel) for EI CVn. The filled circles represent CCD observations.

curve. Assuming the existence of a decrease in the period, a least-squares fitting method yields the following equation,

$$O - C = -0.0015(\pm 0.0001) - 1.24(\pm 0.1) \times 10^{-6}E - 1.11(\pm 0.01) \times 10^{-10}E^2. \quad (2)$$

The corresponding residuals of those light minimum times are listed in Table 3, and shown in the lower panel of Figure 2. After applying the parabolic fitting of the $O - C$ curve, the absolute value of the maximum residual was reduced from 0.0070 for HJD 2451304.8765 to 0.0030 for HJD 2454172.4083, as shown in Table 3. In its upper panel, the solid line was determined by using Equation (2). From the coefficient of the quadratic term, a continuous decrease in the the period, $dP/dt = -3.11(\pm 0.03) \times 10^{-7} \text{ d yr}^{-1}$, can be derived. Due to insufficient data, observing more light minimum times in our future work is needed to identify the nature of the changes in the period.

4 MODELING THE LIGHT CURVE

VR light curves of EI CVn were simultaneously used to deduce the photometric solution using the 2003 version of the Wilson-Devinney (W-D) program with the Kurucz atmospheres (Wilson & Devinney 1971; Wilson 1979, 1990; Kurucz 1993). Because of its spectral type of K5 (Stephenson 1986), the mean effective temperature of the primary star was taken as 5160 K (Cox 2000). The logarithmic bolometric (X and Y) and monochromatic (x and y) limb-darkening coefficients were interpolated from the values of van Hamme (1993). Following Lucy (1967) and Rucinski (1973), the gravity darkening exponents of both components and their bolometric albedo coefficients were set at the values of $g_{1,2} = 4\beta_{1,2} = 0.32$ and $A_{1,2} = 0.5$, respectively, which are appropriate for stars with convective envelopes. The commonly adjustable parameters employed are the orbital inclination i , the mass ratio q , the mean temperature of Star 2 T_2 , the potential of the components Ω_1 , and the monochromatic luminosity of Star 1 L_1 .

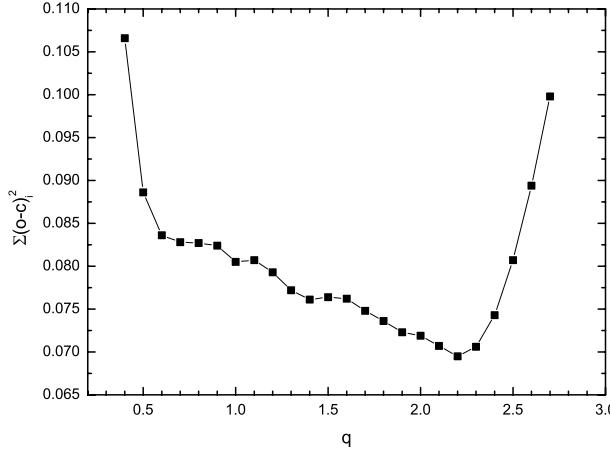


Fig.3 $q - \Sigma$ curve of EI CVn, where a minimum residual of Σ is achieved at $q = 2.2$.

Table 4 Photometric Elements for the Eclipsing Binary EI CVn

Parameters	Unspotted solution	Spotted solution
$i(^{\circ})$	$83.95(\pm 0.39)$	$84.50(\pm 0.36)$
$q = M_s/M_p$	$0.455(\pm 0.004)$	$0.461(\pm 0.003)$
T_p (K)	4410	
X_p, Y_p	0.619, 0.179	
x_{pV}, y_{pV}	0.791, 0.061	
x_{pR}, y_{pR}	0.730, 0.158	
T_s (K)	$4326(\pm 6)$	$4341(\pm 6)$
X_s, Y_s	0.603, 0.199	0.605, 0.195
x_{sV}, y_{sV}	0.789, 0.097	0.789, 0.090
x_{sR}, y_{sR}	0.730, 0.187	0.730, 0.182
$\Omega_p = \Omega_s$	$2.7418(\pm 0.0142)$	$2.7422(\pm 0.0092)$
$L_p/(L_p + L_s)_V$	$0.6374(\pm 0.0016)$	$0.6393(\pm 0.0016)$
$L_p/(L_p + L_s)_R$	$0.6455(\pm 0.0013)$	$0.6460(\pm 0.0013)$
r_p (pole)	$0.4302(\pm 0.0026)$	$0.4313(\pm 0.0017)$
r_p (side)	$0.4597(\pm 0.0035)$	$0.4613(\pm 0.0023)$
r_p (back)	$0.4904(\pm 0.0047)$	$0.4931(\pm 0.0031)$
r_s (pole)	$0.3007(\pm 0.0031)$	$0.3042(\pm 0.0021)$
r_s (side)	$0.3150(\pm 0.0037)$	$0.3190(\pm 0.0025)$
r_s (back)	$0.3535(\pm 0.0064)$	$0.3594(\pm 0.0045)$
$f(%)$	$16.6(\pm 0.9)$	$21.0(\pm 0.7)$
Colatitude ($^{\circ}$)	—	90
Longitude ($^{\circ}$)	—	$239.5(\pm 1.8)$
Radius ($^{\circ}$)	—	$15.87(\pm 2.81)$
Temperature factor	—	$0.87(\pm 0.01)$
$\sum(O - C)_i^2$	0.0700	0.0460

To search for a mass ratio, solutions are obtained for a series of fixed mass ratios from $q = 0.4$ to $q = 2.8$ with an interval of 0.1. For each value of the mass ratio, the calculation started at mode 2 (the detached mode), but the solution always converged to mode 3 (the contact mode). The sum of squared residuals, $\Sigma(O - C)_i^2$, for the corresponding mass ratios is plotted in Figure 3, where a minimum of 0.0695 is achieved at $q = 2.2$. This indicates that EI CVn is a W-type contact binary, i.e., Star 1 (the less massive component, also called the secondary) is eclipsed by Star 2 (the more massive

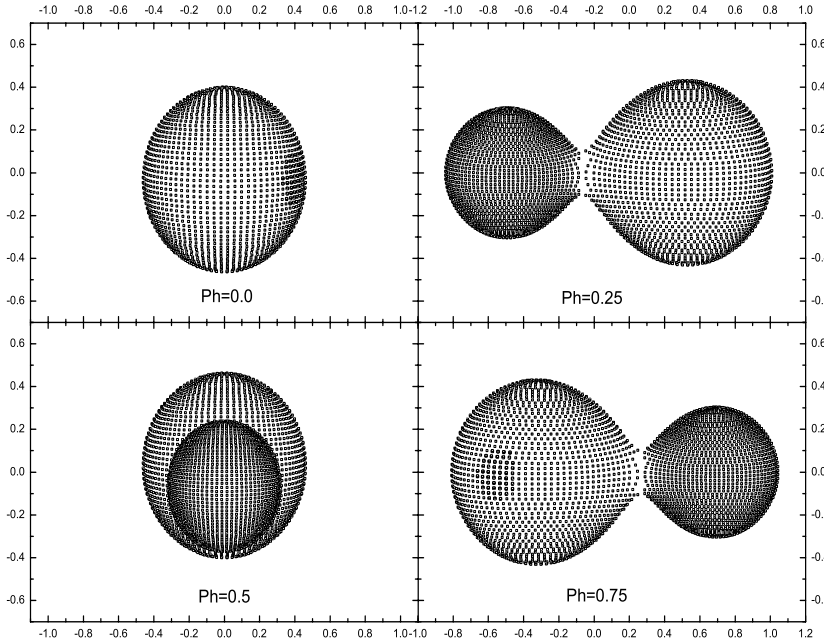


Fig. 4 Geometric configurations of EI CVn at the various phases (0.0, 0.25, 0.5 and 0.75).

component, also called the primary) at the deeper eclipse. At this point, the adjustable parameters were then expanded to include q . When the third light L_3 was set as another free parameter, the solution always yielded a negative value of L_3 . After some iterations, the set of parameters (i , q , Ω , L_p and L_s) were derived, and listed in Table 4. For EI CVn, the asymmetric light curves may result from a cool spot on Star 2 (the primary component). The results of the spotted solution are listed in Table 4. The corresponding theoretical light curves from the spotted solution are shown in Figure 1 as solid lines. The O'Connell effect may be attributed to the activity of star spots. The spot area is up to 1.9% of the area of the more massive component. The overcontact degree of $f = 21.0\%(\pm 0.7\%)$ implies that EI CVn is a weak-contact binary. Moreover, we used the Light Curve (LC) code of the W-D program when modeling the configurations at various phases in Figure 4, where the location of the dark spot is shown as the black area on the more massive component.

5 DISCUSSION

EI CVn is a W-type weak-contact binary with a mass ratio of $q_{ph} = 0.461(\pm 0.003)$ and an overcontact degree of $f = 20.0(\pm 0.7\%)$. From the $O - C$ curve, it is discovered that there exists a weak long-term decrease in the period. This situation appears in many other weak-contact binaries, whose parameters are listed in Table 5. Due to the lack of spectroscopic elements, the absolute parameters of this binary cannot be determined directly. Assuming that the primary is a main-sequence star, its mass could be estimated as $M_p = 0.63M_\odot$, which corresponds to its spectral type K5 (Cox 2000).

The secular period of EI CVn decreases at a rate of $dP/dt = -3.11(\pm 0.03) \times 10^{-7} \text{ d yr}^{-1}$, which is a typical value for this kind of weak-contact binary, as shown in Table 5. Therefore, it is more likely that there exists a decreasing orbital period. This kind of period decrease may generally be explained by the mass transfer from the more massive component to the less massive component.

Table 5 Parameters of Some Weak-contact Binaries with a Period Decrease and a Cyclic Variation

Star	Spectral	Period (d)	q	f (%)	dP/dt (10^{-7} d yr $^{-1}$)	A (d)	P_3 (yr)	Reference
V417 Aql	G0V+F9V	0.3703	0.355	31	-5.50	0.0130	42.4	[1,2]
SS Ari	G0	0.4060	0.308	13	-1.56	0.0205	39.7	[3]
TY Boo	G3	0.3172	0.466	12	-0.30	0.0240	59.7	[4,5]
AO Cam	G0V	0.3299	0.413	12	-1.26	0.0019	7.63	[6, 7, 8]
BS Cas	A-F	0.4408	0.283	31.6	-1.51	0.0023	13.2	[9]
VW Cep	G8V+K0V	0.2783	0.35	22	-7.67	0.0101	30.9	[10]
CC Com	K4/5V	0.2207	0.527	16.7	-0.20	0.0028	23.6	[11,12,13]
EI CVn	K5	0.2608	0.461	20	-3.11	0.0017	4.96	[14]
AP Leo	G0	0.3703	0.297	25	-10.8	0.0049	22.4	[15]
V502 Oph	G2V+F9V	0.4534	0.335	24	-2.88	0.0049	57.9	[16,17,18]
BX Peg	G4.5	0.2804	0.372	23	-9.59	0.0122	52.4	[19]
AH Tau	G1p	0.3327	0.490	10.8	-0.70	0.0171	45.8	[6]
BM UMa	K+K	0.2712	0.54	17	-0.75	0.0101	30.8	[20]

References: [1] Gazeas et al. (2005); [2] Qian (2003); [3] Kim et al. (2003); [4] Yang et al. (2007); [5] Milone et al. (1991); [6] Yang et al. (2010); [7] Rucinski et al. (2000); [8] Baran et al. (2004); [9] Yang et al. (2008); [10] Kaszás et al. (1998); [11] Yang et al. (2009a); [12] Bradstreet (1985); [13] Pribulla et al. (2007); [14] Present work; [15] Qian et al. (2007); [16] Pych et al. (2004); [17] Maceroni et al. (1982); [18] Yüce et al. (2006); [19] Lee et al. (2004); [20] Yang et al. (2009b).

In case of conservative mass transfer, the rate of mass transfer can be calculated via the following well-known formula,

$$\frac{\dot{P}}{P} = 3 \frac{1-q}{q} \frac{\dot{M}_p}{M_p}, \quad (3)$$

where M_p and q represent the mass of the primary and the mass ratio respectively. Inserting the values of \dot{P} , P , M_p and q into Equation (4), the mass transfer rate of EI CVn is $\dot{M}_p = -2.28 \times 10^{-7} M_{\odot} \text{ yr}^{-1}$. With the mass transfer, the separation between both components will decrease. This will result in the shrinkage of the inner and outer critical Lagrangian surfaces, causing the contact degree to increase. Therefore, this kind of weak-contact binary with a decreasing period may evolve into a deep-contact configuration. Moreover, it is necessary for us to obtain many high-precision photometric and spectroscopic observations of EI CVn, in order to better identify the nature of changes in the period and to determine the system's absolute parameters.

Acknowledgements This work was partly supported by the National Natural Science Foundation of China (Grant Nos. 10778707, 10973037 and 10903026). Many thanks are given to the collaborating director Professor J.-Y. Wei for his suggestions and Miss H.-L. Li for her assistance with the observations during the two-year post-doctoral program. New observations of EI CVn were observed using the 60-cm telescope at the Xinglong Station, National Astronomical Observatories, Chinese Academy of Sciences.

References

- Akerlof, C., Amrose, S., Balsano, R., et al. 2000, AJ, 119, 1901
- Baran, A., Zola, S., Rucinski, S. M., et al. 2004, Acta Astron., 54, 195
- Beers, T. C., Bestman, W., & Wilhelm, R. 1994, ApJ, 108, 268
- Blättler, E., & Diethelm, R. 2003, IBVS, 5403, 1
- Bradstreet, D. H. 1985, ApJS, 58, 413
- Cox, A. N. 2000, Allen's Astrophysical Quantities (4th ed.; New York: Springer)
- Davidge, T. J., & Milone, E. F. 1984, ApJS, 55, 571

- Diethelm, R. 2005, IBVS, 5653, 1
 Diethelm, R. 2006, IBVS, 5713, 1
 Diethelm, R. 2007, IBVS, 5781, 1
 Diethelm, R. 2009, IBVS, 5894, 1
 Gazeas, K. D., Baran, A., Niarchos, P., et al. 2005, *Acta Astron.*, 55, 123
 Gettel, S. J., Geske, M. T., & McKay, T. A. 2006, *AJ*, 131, 621
 Hübscher, J., Lehmann, P. B., Monninger G., et al. 2010, IBVS, 5941, 1
 Kaszás, G., Vinkó, J., Szatmáry, K., et al. 1998, *A&A*, 331, 231
 Kim, C.-H., Lee, J. W., Kim, S.-L., et al. 2003, *AJ*, 125, 322
 Kurucz, R. L. 1993, in *ASP Conf. Ser.*, 44, 87
 Kwee, K. K., & van Woerden, H. 1956, *Bull. Astron. Inst. Netherlands*, 12, 327
 Lee, J. W., Kim, C.-H., Han W., et al. 2004, *MNRAS*, 352, 1041
 Li, H.-L., Yang, Y.-G., Su, W., Wang, H.-J., & Wei, J.-Y. 2009, *RAA (Research in Astronomy and Astrophysics)*, 9, 1035
 Lucy, L. B. 1967, *Z. Astrophys.*, 65, 89
 Maceroni, C., Milano, L., & Russo, G. 1982, *A&AS*, 49, 123
 Milone, E. E. 1968, *AJ*, 73, 708
 Milone, E. F., Groisman, G., Fry, D. J. I., & Bradstreet, D. H. 1991, *AJ*, 370, 677
 Nelson, R. H. 2009, IBVS, 5875, 1
 Pribulla, T., Rucinski, S. M., Conidis, G., et al. 2007, *AJ*, 133, 1997
 Pych, W., Rucinski, S. M., DeBond, H., et al. 2004, *AJ*, 127, 1712
 Qian, S.-B. 2003, *A&A*, 400, 649
 Qian, S.-B., Xiang, F.-Y., Zhu, L.-Y., et al. 2007, *AJ*, 133, 357
 Rucinski, S. M. 1973, *Acta Astron.*, 23, 79
 Rucinski, S. M., Lu, W., & Mochnacki, S. M. 2000, *AJ*, 120, 1133
 Stephenson, C. B. 1986, *AJ*, 91, 144
 van Hamme, W. 1993, *AJ*, 106, 2096
 Wilson, R. E. 1979, *ApJ*, 234, 1054
 Wilson, R. E. 1990, *ApJ*, 356, 613
 Wilson, R. E., & Devinney, E. J. 1971, *ApJ*, 166, 605
 Yang, Y.-G., Dai, J.-M., Yin, X.-G., & Xiang, F.-Y. 2007, *AJ*, 134, 179
 Yang, Y.-G., Lü, G.-L., Yin, X.-G., et al. 2009a, *AJ*, 137, 236
 Yang, Y.-G., Wei, J.-Y., & He, J.-J. 2008, *AJ*, 136, 594
 Yang, Y.-G., Wei, J.-Y., Kreiner, J. M., & Li, H.-L. 2010, *AJ*, 139, 195
 Yang, Y.-G., Wei, J.-Y., & Nakajiam, K. 2009b, *PASJ*, 61, 13
 Yüce, K., Selam, S. O., Albayrak, B., & Ak, T. 2006, *Ap&SS*, 304, 67